Available online at www.sciencedirect.com
ScienceDirect
Journal of Sound and Vibration 322 (2009) 1100–1116
JOURNAL OF SOUND AND VIBRATION
www.elsevier.com/locate/jsvi

Effect of crack on drilling vibration

Bo-Wun Huang[a,*], Jao-Hwa Kuang[b], Pu-Ping Yu[a]

[a]Department of Mechanical Engineering, Cheng Shiu University, 840 Cheng Ching Rd., Niaosung, 833 Kaohsiung, Taiwan
[b]Department of Mechanical and Electromechanical Engineering, National Sun Yat-Sen University, Kaohsiung, Taiwan

Received 15 November 2007; received in revised form 13 May 2008; accepted 30 November 2008
Handling Editor: L.G. Tham
Available online 20 January 2009

Abstract

Effect of drill parameters and the local crack on the dynamic characteristics of a drill during the drilling through process is investigated in this study. A pre-twisted beam with a local crack is used to simulate the cracked drill. The release energy model is employed to characterize the stiffness variation around the crack. A moving Winkler-type elastic foundation assumption is used to approximate the time dependent work piece stiffness distribution on rotating drill during the drilling process. In this article, a drill vibration model with time varied boundary condition is presented. The effects of cracks, rotational speed, pre-twisted angle and thrust force on the vibration of drill are considered. A serious vibration is observed at the moment as the drill touch the work piece in a drilling process. The simulated results also indicate that the local crack may aggravate the vibration.

1. Introduction

Drilling is used widely in different manufactures. However, many parameters may affect the drilling performance. So how to control these drilling parameters to provide the reliable and high quality drilling is very important in much mass production. To improve the drilling performance and reliability the vibration variation in the drilling process is studied. In this study, the effects of rotation speed, drill shape parameters, thrust force and local crack on the drill vibration are considered.

The most common cause of drill failure is breakage. Drill breakage usually occurs because of excessive drilling force and vibration in the drilling process [1]. Only a few studies have been conducted on dynamic drilling process. Even if a given property leads to undesirable effects such as chatter and drill breakage, etc., few investigators have turned their attention to this problem; presumably because such effects are always believed to be caused by the drill structure. Traditional drilling analysis has always focused on the drill itself, such as Refs. [2–5]. The different pre-twisted beams have been used to model the drill in a number of papers [2,3,6,7]. The effects of pre-twisted angle and rotation speed on the drilling vibration were analyzed. The buckling load and natural frequency of a drill bit were also investigated, as Refs. [8–10].

Cyclic fatigue during operation frequently causes cracks to appear in a drill, [11–14], especially when drilling composite, ceramic materials and micro holes. Cracks near the roots of the drill may change the local

*Corresponding author. Fax: +886 7 7310213.
E-mail address: huangbw@csu.edu.tw (B.-W. Huang).

0022-460X/$ - see front matter © 2008 Elsevier Ltd. All rights reserved.
doi:10.1016/j.jsv.2008.11.048

flexibility and introduce so-called irregular local structures. Local cracks might affect the system's dynamic behavior and also cause severe drill breakage. This study examines the effect of the crack depth on the dynamic characteristics of a drill while drilling through a work piece. During the preceding two decades, a number of studies [15–21] reported that cracks might change the vibration behavior of a structural system.

Mathematical models on complex drill bits to estimate the natural frequencies or cutting properties were investigated by the previous researchers. The effects of complex geometry or the cutting chip on the cutting and dynamic drill bit properties were examined. Even a small variation in the geometry or symmetry could produce a very strong influence on the cutting and dynamic properties of a drill, as in Ref. [22]. Such models can provide useful information for drill bit design. In this paper, the focus is a time dependent drilling process. Hence, considering a drill with a moving boundary is unavoidable. Recently, a structural system with moving masses, forces and boundaries was developed for these investigations, [23–27]. In actual engineering, the work piece restricts the vibration of drill as this drill goes into this work piece is found. For the above reason, the simple spring stiffness is employed to simulate the restriction for drill. Because of the cutting depth increasing by time, the moving elastic foundation is also used to simulate the drilling process constraint. For this simulation, it is aim to attempt to explain that the large vibration of the drill as this drill just drilling into a work piece is found. From the numerical and experimental analysis results in this article, it is justified that the assumption model can be employed to simulate the drilling process.

Before the drill tip touches the work piece no axial drilling load has considered. However, a time dependent axial load introduced at the drill tip is employed to model the dynamic response of the drill during the drilling through process. In the proposed model, the time dependent moving elastic foundation is also used to characterize the interaction between the drill and the work piece at different drill depth. In other words, in practical, the work piece restricts the vibration of drill as the drill goes into this work piece. To include this constriction effect on the drill in drilling modeling, the uniform spring stiffness is employed in this study. The proposed model is aim to explore the effect of axial stiffness variation on the dynamic response of a drill during the drilling process. The moving elastic foundation is used to simulate the constraint on the drill during the drilling process. In an actual drilling process, it is observed frequently that the drill is fractured at the moment as the drill start to penetrate into a work piece. The variation of drilling force, especially the thrust force, in the drilling process will dominate the drill dynamic characteristics. For the sake of convenience, the time dependent thrust force $P[u_s(t-t^*)-u_s(t-t^{**})]$, axial force, is used to simulate the applied drilling force, where $u_s(\,)$ is the unit step function. The variation of drilling boundary condition during the drilling process is considered in the equation of motion. Two moving Winkler-type elastic foundations are used to simulate the time dependent boundary between the drill surface and the drilled work piece surfaces. The aim of this study is to examine the time dependent transverse vibrations during the drilling process. The effect of a local crack on the vibration of a drill during the drilling process was also studied.

2. Theory and formulations

According to Ref. [28], little difference was found between the complex and rectangular cross-sections on dynamic drill characteristics and a pre-twisted beam with a rectangular cross-section is proposed to simulate a drill. The drill, a cantilever pre-twisted beam, with rotational speed Ω is illustrated in Fig. 1(a). The length of the drill is L. The symbols t_0 and b are the thickness and breadth of the drill, respectively. The deflection components $v(r,t)$ and $u(r,t)$ denote the transverse flexible deflections of the drill in the x and y directions.

The equation of motion, which is derived as Appendix A, for the drill body is given by

$$\frac{\partial^2}{\partial r^2}\left(EI_{yy}\frac{\partial^2 u}{\partial r^2}+EI_{xy}\frac{\partial^2 v}{\partial r^2}\right)-\frac{\partial}{\partial r}\left(\bar{I}_{yy}\frac{\partial^3 u}{\partial t^2\partial r}+\bar{I}_{xy}\frac{\partial^3 v}{\partial t^2\partial r}\right)+\mu\frac{\partial^2 u}{\partial t^2}-2\mu\Omega\frac{\partial v}{\partial t}-\mu\Omega^2 u=0 \tag{1}$$

$$\frac{\partial^2}{\partial r^2}\left(EI_{xx}\frac{\partial^2 v}{\partial r^2}+EI_{xy}\frac{\partial^2 u}{\partial r^2}\right)-\frac{\partial}{\partial r}\left(\bar{I}_{xx}\frac{\partial^3 v}{\partial t^2\partial r}+\bar{I}_{xy}\frac{\partial^3 u}{\partial t^2\partial r}\right)+\mu\frac{\partial^2 v}{\partial t^2}+2\mu\Omega\frac{\partial u}{\partial t}-\mu\Omega^2 v=0 \tag{2}$$

where $\mu=\rho b t_0$.

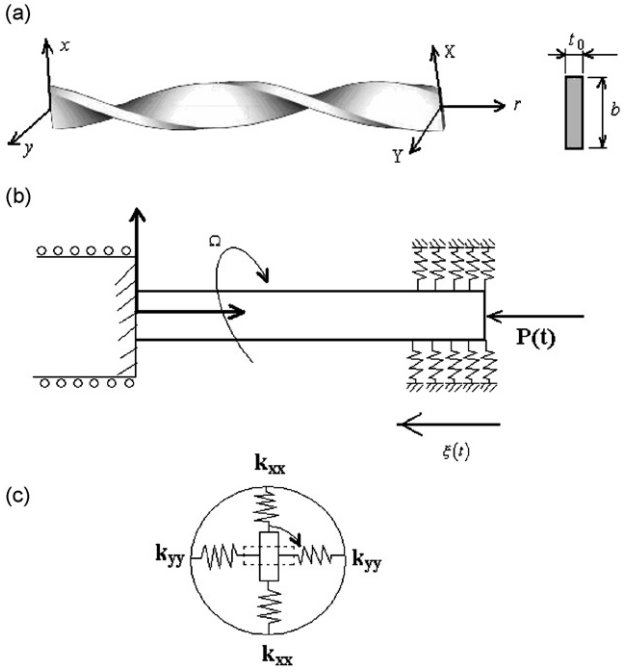

Fig. 1. A sketch of a drill in drilling process: (a) the schematic diagram of the body for micro drill and (b) the time dependent drilling process model.

This drill is considered pre-twisted with a uniform twist angle of β. The area moments of inertia at position r can then be derived as

$$I_{xx} = I^{XX}\cos^2\left(\frac{r}{L}\beta\right) + I^{YY}\sin^2\left(\frac{r}{L}\beta\right) \tag{3}$$

$$I_{yy} = I^{XX}\sin^2\left(\frac{r}{L}\beta\right) + I^{YY}\cos^2\left(\frac{r}{L}\beta\right) \tag{4}$$

$$I_{xy} = (I^{YY} - I^{XX})\sin\left(\frac{r}{L}\beta\right)\cos\left(\frac{r}{L}\beta\right) \tag{5}$$

where

$$I^{XX} = \frac{bt_0^3}{12} \tag{6}$$

$$I^{YY} = \frac{b^3 t_0}{12} \tag{7}$$

and

$$\bar{I}_{xx} = \bar{I}^{XX}\cos^2\left(\frac{r}{L}\beta\right) + \bar{I}^{YY}\sin^2\left(\frac{r}{L}\beta\right) \tag{8}$$

$$\bar{I}_{yy} = \bar{I}^{XX}\sin^2\left(\frac{r}{L}\beta\right) + \bar{I}^{YY}\cos^2\left(\frac{r}{L}\beta\right) \tag{9}$$

$$\bar{I}_{xy} = (\bar{I}^{YY} - \bar{I}^{XX})\sin\left(\frac{r}{L}\beta\right)\cos\left(\frac{r}{L}\beta\right) \tag{10}$$

The above notations $\bar{I}^{XX}$ and $\bar{I}^{YY}$ are the principal mass moments of inertia. The corresponding boundary conditions are

$$\delta\left(\frac{\partial u}{\partial r}\right)=0 \quad \text{or} \quad EI_{yy}\frac{\partial^2 u}{\partial r^2}+EI_{xy}\frac{\partial^2 v}{\partial r^2}=0 \tag{11}$$

$$\delta\left(\frac{\partial v}{\partial r}\right)=0 \quad \text{or} \quad EI_{xx}\frac{\partial^2 v}{\partial r^2}+EI_{xy}\frac{\partial^2 u}{\partial r^2}=0 \tag{12}$$

$$\delta u=0 \quad \text{or} \quad \bar{I}_{yy}\frac{\partial^3 u}{\partial t^2\partial r}+\bar{I}_{xy}\frac{\partial^3 v}{\partial t^2\partial r}-\frac{\partial}{\partial r}\left(EI_{yy}\frac{\partial^2 u}{\partial r^2}+EI_{xy}\frac{\partial^2 v}{\partial r^2}\right)=0 \tag{13}$$

$$\delta v=0 \quad \text{or} \quad \bar{I}_{xx}\frac{\partial^3 v}{\partial t^2\partial r}+\bar{I}_{xy}\frac{\partial^3 u}{\partial t^2\partial r}-\frac{\partial}{\partial r}\left(EI_{xx}\frac{\partial^2 v}{\partial r^2}+EI_{xy}\frac{\partial^2 u}{\partial r^2}\right)=0 \tag{14}$$

The above boundary conditions are similar in author's previous investigation [29]. For the solution of above equation, the comparison functions must satisfy the boundary conditions and are displayed as follows, [30,31]:

$$u_s=v_s=u_s'=v_s'=0 \quad \text{at } r=0 \tag{15}$$

$$u_s''=v_s''=u_s'''=v_s'''=0 \quad \text{at } r=L \tag{16}$$

where the symbol prime ($'$) denotes the partial derivative with respect to r.

2.1. Drill body with a crack

A crack initiated on the drill body located at $r=r^c$ is considered. For simplicity, this open crack model, as proposed in Refs. [33,34], is employed in this study to simulate the drill crack in the weakest direction (the v transverse displacement is considered). Generally speaking, this assumption will not affect the calculation of the natural frequencies and the corresponding mode shapes in u displacement. According to the investigations in Refs. [32,33], elastic deformation energy in alterations in places in the crack caused by the bending moment is the only important change in the case of slender beams. Therefore, the released energy in this crack may be written in the form:

$$U_{\xi}^{c}=b\int_0^a \frac{(1-\mu^2)}{E}K_I^2\,\mathrm{d}a \tag{17}$$

where a, μ are the depth of the crack and the Poisson's ratio of the drill. K_I is the stress intensity factor under a mode I load. In this case, the mode I stress intensity factor K_I can be approximated using Eq. [17] as

$$K_I=\frac{6p_b}{t_0^2 b}\sqrt{\pi(a/t_0)t_0}F_I(a/t_0) \tag{18}$$

where

$$p_b=EI_{xx}v''|_{r=r^c} \tag{19}$$

$$F_I(a/t_0)=\sqrt{\frac{2}{\pi(a/t_0)}\tan\left(\frac{\pi(a/t_0)}{2}\right)}\frac{0.923+0.199\left[1-\sin\left(\frac{\pi(a/t_0)}{2}\right)\right]^4}{\cos\left(\frac{\pi(a/t_0)}{2}\right)} \tag{20}$$

Adapting Eq. (17) gives

$$U_{\xi}^{c}=3E(1-\mu^2)t_0\int_0^L I_3^{xx}Q\left(\frac{a}{t_0}\right)[v_3''(r,t)|_{r=r^c}]^2\,\mathrm{d}r \tag{21}$$

and

$$Q(a/t_0) = \int_0^{a/t_0} \pi(a/t_0) F_I^2(a/t_0) d(a/t_0) \tag{22}$$

Similarly, using Hamilton's principle, the equations of motion can be derived for the cracked drill. This leads to

$$\frac{\partial^2}{\partial r^2}\left(EI_{yy}\frac{\partial^2 u}{\partial r^2} + EI_{xy}\frac{\partial^2 v}{\partial r^2}\right) - \frac{\partial}{\partial r}\left(\bar{I}_{yy}\frac{\partial^3 u}{\partial t^2 \partial r} + \bar{I}_{xy}\frac{\partial^3 v}{\partial t^2 \partial r}\right) + \mu\frac{\partial^2 u}{\partial t^2} - 2\mu\Omega\frac{\partial v}{\partial t} - \mu\Omega^2 u = 0 \tag{23}$$

In the v displacement, as $r = (0, r^c) \cup (r^c, L)$:

$$\frac{\partial^2}{\partial r^2}\left(EI_{xx}\frac{\partial^2 v}{\partial r^2} + EI_{xy}\frac{\partial^2 u}{\partial r^2}\right) - \frac{\partial}{\partial r}\left(\bar{I}_{xx}\frac{\partial^3 v}{\partial t^2 \partial r} + \bar{I}_{xy}\frac{\partial^3 u}{\partial t^2 \partial r}\right) + \mu\frac{\partial^2 v}{\partial t^2} + 2\mu\Omega\frac{\partial u}{\partial t} - \mu\Omega^2 v = 0 \tag{24}$$

In the v displacement, as $r = r^c$:

$$\frac{\partial^2}{\partial r^2}\left(EI_{xx}\frac{\partial^2 v}{\partial r^2} + EI_{xy}\frac{\partial^2 u}{\partial r^2}\right) - \frac{\partial}{\partial r}\left(\bar{I}_{xx}\frac{\partial^3 v}{\partial t^2 \partial r} + \bar{I}_{xy}\frac{\partial^3 u}{\partial t^2 \partial r}\right) - 6EI_{xx}(1-\mu^2)t_0 Q(\bar{\gamma})[v'']'' + \mu\frac{\partial^2 v}{\partial t^2} + 2\mu\Omega\frac{\partial u}{\partial t} - \mu\Omega^2 v = 0 \tag{25}$$

2.2. Drilling through the work piece

An investigation of a drill with a crack in a drilling process is presented in this article. In the mathematical sense, a time dependent boundary and thrust force can be employed to simulate this drilling process. Hence, the moving boundary and time dependent thrust force are employed in this article. To make the moving boundary more convenient, two moving Winkler-type elastic foundations [34] were used to simulate the time dependent boundary, as shown in Fig. 1(b). From the above, the uniform distribution stiffness k_{xx} and k_{yy} can be modeled as these types of elastic foundations. Fig. 1(b) also shows the drilling process model. First of all, a conservative compressive force, $P[u_s(t-t^*)-u_s(t-t^{**})]$, is applied at the free end of the drill as it drills through the work piece. The work performed by this thrust force as the drill deforms is derived in

$$W_p(t) = \int_0^L \frac{1}{2} P u_s(t-t^*)\left[\left(\frac{\partial u(r,t)}{\partial r}\right)^2 + \left(\frac{\partial v(r,t)}{\partial r}\right)^2\right] dr - \int_0^L \frac{1}{2} P u_s(t-t^{**})\left[\left(\frac{\partial u(r,t)}{\partial r}\right)^2 + \left(\frac{\partial v(r,t)}{\partial r}\right)^2\right] dr \tag{26}$$

where $u_s(\,)$ is the unit step function. The exact drilling time is denoted as t^* and t^{**} is the time for the drilling throughout the work piece. The moving boundary constraints are also considered. Without considering the moving boundary effects introduced from the time varying drilling depth, the strain energy due to the Winkler-type elastic foundations can be derived [34] as

$$U_k(t) = 2\int_0^L \left[\frac{1}{2}k_{xx}u^2(r,t) + \frac{1}{2}k_{yy}v^2(r,t)\right] dr \tag{27}$$

In this work, the unit step function $u_s(t-t^*)$ is employed to distinguish the effect of Winkler-type elastic foundation in different drill periods, i.e. before the drill touch the work piece, during the drilling or after the drill goes through the work piece. If the drilling time and moving boundary effects are considered, the above strain energy is

$$U_k(t) = 2\int_0^L \left[\frac{1}{2}k_{xx}u_s(r-r^*)u_s(t-t^*)u^2(r,t) + \frac{1}{2}k_{yy}u_s(r-r^*)u_s(t-t^*)v^2(r,t)\right] dr - 2\int_0^L \left[\frac{1}{2}k_{xx}u_s(r-r^{**})u_s(t-t^{**})u^2(r,t) + \frac{1}{2}k_{yy}u_s(r-r^{**})u_s(t-t^{**})v^2(r,t)\right] dr \tag{28}$$

where

$$r^*(t) = L - f \times (t - t^*)u_s(t - t^*) \tag{29}$$

$$r^{**}(t) = L - f \times (t - t^{**})u_s(t - t^{**}) \tag{30}$$

As above, these time dependent thrust force and moving boundary constraints are considered in the above equations. For the sake of convenience, the notation $\xi(t)$ is used to denote the drilling displacement. This non-dimensionless drilling displacement is written as follows:

$$\xi(t) = \frac{f \times (t - t^*)u_s(t - t^*)}{L} \tag{31}$$

If the drill drills throughout a work piece, the above displacement is rewritten as

$$\xi(t) = \frac{f \times (t - t^*)u_s(t - t^*)}{L} - \frac{f \times (t - t^{**})u_s(t - t^{**})}{L} \tag{32}$$

where f is the drill feed velocity.

Both the time dependent thrust force and boundary are investigated. Hence, the equation of motion for the drill drilling throughout work piece can be rewritten as follows:

$$\begin{aligned}
&\frac{\partial^2}{\partial r^2}\left(EI_{yy}\frac{\partial^2 u}{\partial r^2} + EI_{xy}\frac{\partial^2 v}{\partial r^2}\right) - \frac{\partial}{\partial r}\left(\bar{I}_{yy}\frac{\partial^3 u}{\partial t^2 \partial r} + \bar{I}_{xy}\frac{\partial^3 v}{\partial t^2 \partial r}\right) + Pu_s(t - t^*)\frac{\partial^2 u}{\partial r^2} \\
&\quad - Pu_s(t - t^{**})\frac{\partial^2 u}{\partial r^2} + 2k_{xx}u_s(r - r^*(t))u_s(t - t^*)u \\
&\quad - 2k_{xx}u_s(r - r^{**}(t))u_s(t - t^{**})u + \mu\frac{\partial^2 u}{\partial t^2} - 2\mu\Omega\frac{\partial v}{\partial t} - \mu\Omega^2 u = 0
\end{aligned} \tag{33}$$

In the v displacement, as $r = (0, r^c) \cup (r^c, L)$:

$$\begin{aligned}
&\frac{\partial^2}{\partial r^2}\left(EI_{xx}\frac{\partial^2 v}{\partial r^2} + EI_{xy}\frac{\partial^2 u}{\partial r^2}\right) - \frac{\partial}{\partial r}\left(\bar{I}_{xx}\frac{\partial^3 v}{\partial t^2 \partial r} + \bar{I}_{xy}\frac{\partial^3 u}{\partial t^2 \partial r}\right) + Pu_s(t - t^*)\frac{\partial^2 v}{\partial r^2} \\
&\quad - Pu_s(t - t^{**})\frac{\partial^2 v}{\partial r^2} + 2k_{yy}u_s(r - r^*(t))u_s(t - t^*)v \\
&\quad - 2k_{yy}u_s(r - r^{**}(t))u_s(t - t^{**})v + \mu\frac{\partial^2 v}{\partial t^2} + 2\mu\Omega\frac{\partial u}{\partial t} - \mu\Omega^2 v = 0
\end{aligned} \tag{34}$$

In the v displacement, as $r = r^c$:

$$\begin{aligned}
&\frac{\partial^2}{\partial r^2}\left(EI_{xx}\frac{\partial^2 v}{\partial r^2} + EI_{xy}\frac{\partial^2 u}{\partial r^2}\right) - \frac{\partial}{\partial r}\left(\bar{I}_{xx}\frac{\partial^3 v}{\partial t^2 \partial r} + \bar{I}_{xy}\frac{\partial^3 u}{\partial t^2 \partial r}\right) + Pu_s(t - t^*)\frac{\partial^2 v}{\partial r^2} \\
&\quad - Pu_s(t - t^{**})\frac{\partial^2 v}{\partial r^2} - 6EI_{xx}(1 - \mu^2)t_0 Q(\bar{\gamma})[v'']'' \\
&\quad + 2k_{yy}u_s(r - r^*(t))u_s(t - t^*)v - 2k_{yy}u_s(r - r^{**}(t))u_s(t - t^{**})v \\
&\quad + \mu\frac{\partial^2 v}{\partial t^2} + 2\mu\Omega\frac{\partial u}{\partial t} - \mu\Omega^2 v = 0
\end{aligned} \tag{35}$$

Solutions for the eigenvalue problem are expressed as

$$u(r, t) = \sum_{i=1}^{m} p_i(t)\phi_i(r) \tag{36}$$

$$v(r, t) = \sum_{i=1}^{m} q_i(t)\phi_i(r) \tag{37}$$

where $\phi_i(r)$ are the comparison functions for Eqs. (33)–(35) and $p_i(t)$, $q_i(t)$ are the corresponding weighting coefficients, which are to be determined. These comparison functions are displayed as follows:

$$\phi_i(r) = (\cosh\ \lambda_i r - \cos\ \lambda_i r) - \frac{\cos\ \lambda_i + \cosh\ \lambda_i}{\sin\ \lambda_i + \sinh\ \lambda_i}(\sinh\ \lambda_i r - \sin\ \lambda_i r) \tag{38}$$

and

$$\cos\lambda_i r \cosh\lambda_i r + 1 = 0 \quad \text{for } i = 1, 2, \ldots, m \tag{39}$$

By applying Galerkin's method, the equations of motion for the drill can be derived in matrix form as

$$[M]\begin{Bmatrix}\ddot{p}\\ \ddot{q}\end{Bmatrix} + 2\Omega[G]\begin{Bmatrix}\dot{p}\\ \dot{q}\end{Bmatrix} + \{[\mathrm{K}]_a + [Pu_s(t-t^*) - Pu_s(t-t^{**})][K]_b + \Omega^2[K]_c + [u_s(r-r^{**}(t))u_s(t-t^{**}) - u_s(r-r^{**}(t))u_s(t-t^{**})][K]_d - [K]_e\}\begin{Bmatrix}p\\ q\end{Bmatrix} = 0 \tag{40}$$

where

$$[M] = \begin{bmatrix}[M]^1 + [M]^2 & [M]^4\\ [M]^4 & [M]^1 + [M]^2\end{bmatrix} \tag{41}$$

$$[G] = \begin{bmatrix}[0] & -[M]^1\\ [M]^1 & 0\end{bmatrix} \tag{42}$$

$$[K]_a = \begin{bmatrix}[K]^1 & [K]^3\\ [K]^3 & [K]^2\end{bmatrix} \tag{43}$$

$$[K]_b = \begin{bmatrix}-[K]^4 & [0]\\ [0] & -[K]^4\end{bmatrix} \tag{44}$$

$$[K]_c = \begin{bmatrix}-[M]^1 & [0]\\ [0] & -[M]^1\end{bmatrix} \tag{45}$$

$$[K]_d = \begin{bmatrix}2k_{xx}[K]^5 & [0]\\ [0] & 2k_{yy}[K]^5\end{bmatrix} \tag{46}$$

$$[K]_e = \begin{bmatrix}[0] & [0]\\ [0] & [K]^6\end{bmatrix} \tag{47}$$

These matrices are illustrated in detail as follows:

$$M_{ij} = \int_0^1 \mu\phi_i(\bar{r})\phi_j(\bar{r})\,\mathrm{d}\bar{r} \tag{48}$$

$$M_{ij}^2 = \frac{\bar{I}_{yy}}{L^2}\int_0^1 \frac{\mathrm{d}\phi_i(\bar{r})}{\mathrm{d}\bar{r}}\frac{\mathrm{d}\phi_j(\bar{r})}{\mathrm{d}\bar{r}}\,\mathrm{d}\bar{r} \tag{49}$$

$$M_{ij}^3 = \frac{\bar{I}_{xx}}{L^2}\int_0^1 \frac{\mathrm{d}\phi_i(\bar{r})}{\mathrm{d}\bar{r}}\frac{\mathrm{d}\phi_j(\bar{r})}{\mathrm{d}\bar{r}}\,\mathrm{d}\bar{r} \tag{50}$$

$$M_{ij}^4 = \frac{\bar{I}_{xy}}{L^2}\int_0^1 \frac{\mathrm{d}\phi_i(\bar{r})}{\mathrm{d}\bar{r}}\frac{\mathrm{d}\phi_j(\bar{r})}{\mathrm{d}\bar{r}}\,\mathrm{d}\bar{r} \tag{51}$$

$$K_{ij}^1 = \frac{E}{L^4}\int_0^1 I_{yy}\frac{\mathrm{d}^2\phi_i(\bar{r})}{\mathrm{d}\bar{r}^2}\frac{\mathrm{d}^2\phi_j(\bar{r})}{\mathrm{d}\bar{r}^2}\,\mathrm{d}\bar{r} \tag{52}$$

$$K_{ij}^2 = \frac{E}{L^4}\int_0^1 I_{xx}\frac{\mathrm{d}^2\phi_i(\bar{r})}{\mathrm{d}\bar{r}^2}\frac{\mathrm{d}^2\phi_j(\bar{r})}{\mathrm{d}\bar{r}^2}\,\mathrm{d}\bar{r} \tag{53}$$

$$K_{ij}^3 = \frac{EI_{xy}}{L^4}\int_0^1 \frac{\mathrm{d}^2\phi_i(\bar{r})}{\mathrm{d}\bar{r}^2}\frac{\mathrm{d}^2\phi_j(\bar{r})}{\mathrm{d}\bar{r}^2}\,\mathrm{d}\bar{r} \tag{54}$$

$$K_{ij}^4 = \frac{1}{L^2}\int_0^1 \frac{\mathrm{d}\phi_i(\bar{r})}{\mathrm{d}\bar{r}}\frac{\mathrm{d}\phi_j(\bar{r})}{\mathrm{d}\bar{r}}\,\mathrm{d}\bar{r} \tag{55}$$

$$K_{ij}^5 = \int_0^1 \phi_i(\bar{r})\phi_j(\bar{r})\,\mathrm{d}\bar{r} \tag{56}$$

$$K_{ij}^6 = 6\frac{EI_{xx}}{L^4}(1-\mu^2)\left(\frac{t_0}{L}\right)Q(\bar{\gamma})[\phi_i''(\bar{r})\phi_j''(\bar{r})]_{r=r^c} \tag{57}$$

Table 1
The difference in the first natural frequencies of the pre-twisted beams solved by different methods.

Pre-twisted angle (deg)	Tekinalp and Ulsoy [4]	Liao and Dang [6]	Proposed
0	3.516	3.516	3.516
45	3.551	3.551	3.541
90	3.586	3.621	3.614

Non-dimensional frequency. $L = 100\,\mathrm{cm}$, $t_0 = 0.5\,\mathrm{cm}$, $b = 8\,\mathrm{cm}$.

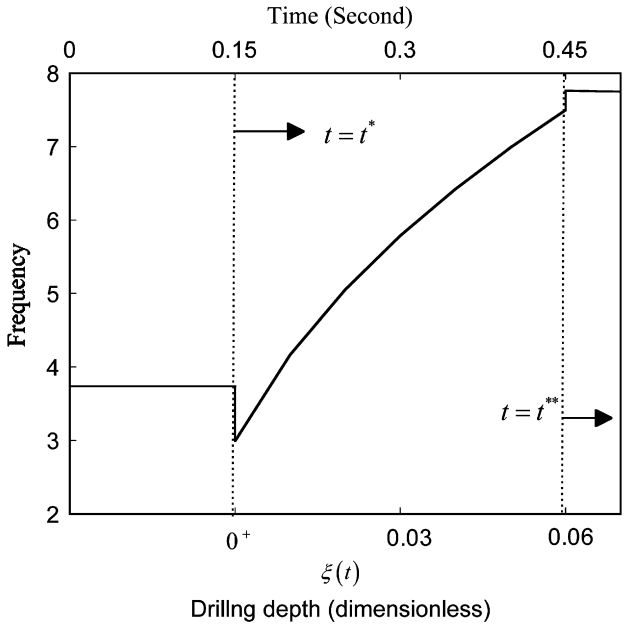

Fig. 2. Natural frequencies of a drill in drilling through a work piece ($f = 0.002\,\mathrm{m/s}$, $\bar{\Omega} = 0.5$, $P = 1500\,\mathrm{N}$, $\beta = 31.416\,\mathrm{rad/m}$).

where

$$\bar{r} = \frac{r}{L} \tag{58}$$

$$\bar{r}^{*}(t) = \frac{r^{*}(t)}{L} \tag{59}$$

$$\bar{r}^{**}(t) = \frac{r^{**}(t)}{L} \tag{60}$$

3. Results and discussion

The vibrations of a drill while drilling through a work piece are investigated. In this article, the geometric parameters of the drill are $(t/L) = 0.005$, $(b/L) = 0.01$ and $\beta = 31.416\,\text{rad/m}$. According to Ref. [28], in the drilling process the thrust load $P = 3000\,\text{N}$, feeding speed $f = 0.002\,\text{m/s}$, $r^{c} = 0.0$, $\bar{\Omega} = 0.5$ and

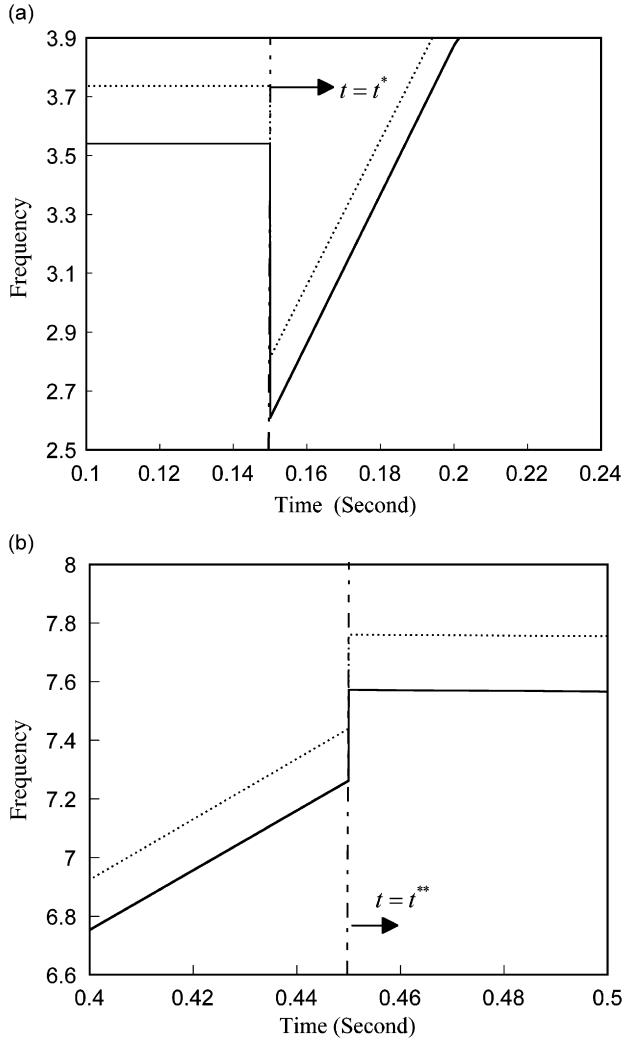

Fig. 3. Natural frequencies of a drill in drilling through a work piece with or without a crack: (a) drilling into a work piece, (b) drilling throughout a work piece. ····· without cracks $\gamma = 0.0$, ——— with a crack $\gamma = 0.2$.

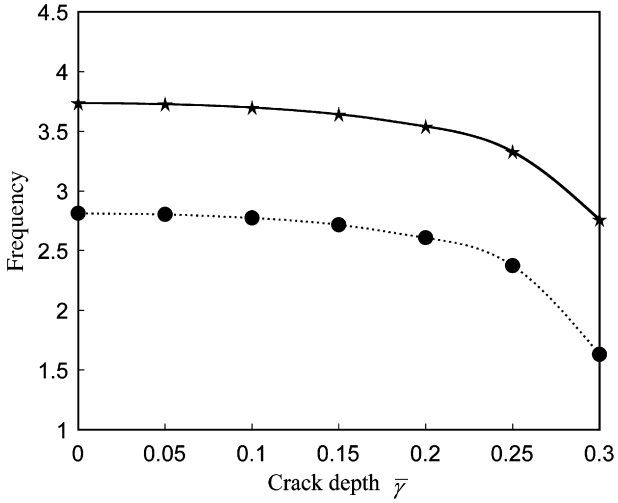

Fig. 4. Natural frequencies of a drill in drilling process with different crack depths. ····· just drilling, ——— undrilling.

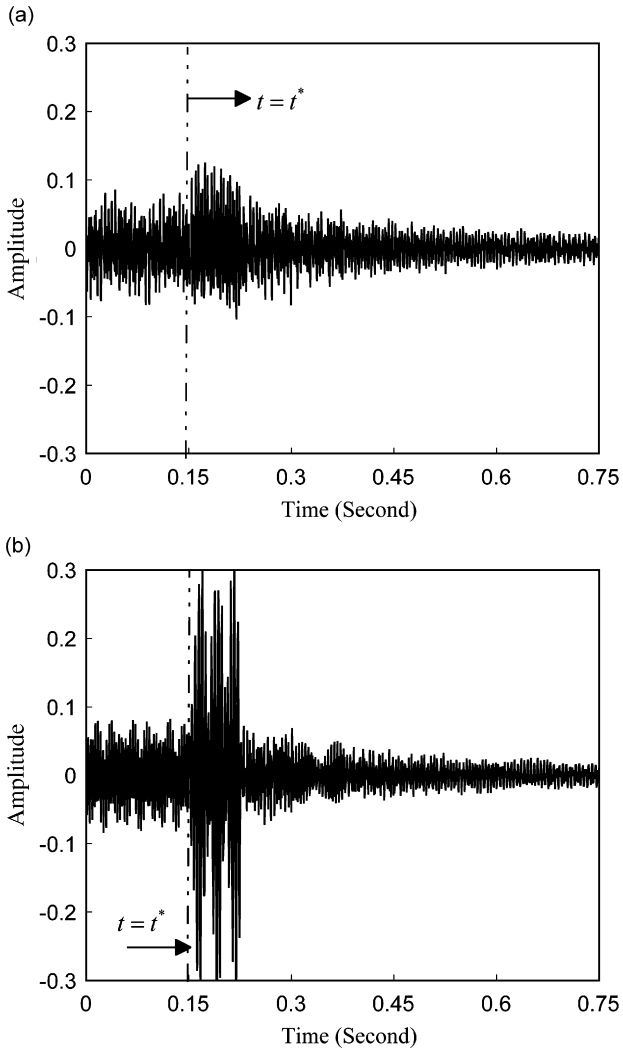

Fig. 5. Time responses of a drill in the drilling process with or without a crack, exciting frequency $\bar{\omega} = 2.0$: (a) without cracks $\gamma = 0.0$ and (b) with a crack $\gamma = 0.3$.

$k_{xx} = k_{yy} = 1 \times 10^8\,\mathrm{N/m^2}$ were considered. As to our knowledge, there is no similar drilling process model was proposed. The finite element solutions of pre-twisted beams were employed to solve the distribution of natural frequencies of a drill in studies [4,6]. However, in this study, the exact mode shape functions of a straight beam were considered as the comparison functions to solve the equations of motion. Therefore, the basic assumption made in this modeling is that the flexibility of the pre-twisted beam is not different too much from the straight beam. Table 1 lists the difference in the first natural frequency calculated by using the methods proposed in the previous investigations [4,6] and the results simulated from the proposed model. The good agreement between solved natural frequencies indicated that the proposed model is feasible to analyze the dynamic responses of a drill during the drilling process with acceptable accuracy.

The effects of drill parameters and crack are the most important parameters on drilling vibration in drilling process. Most studies investigated the drill structure, drilling chips and drilling force. Few investigations, [35], paid attention to the dynamic properties in the drilling process, especially while drilling through a work piece and with a crack. For the drilling process, this article presents the time dependent vibrations of a drill.

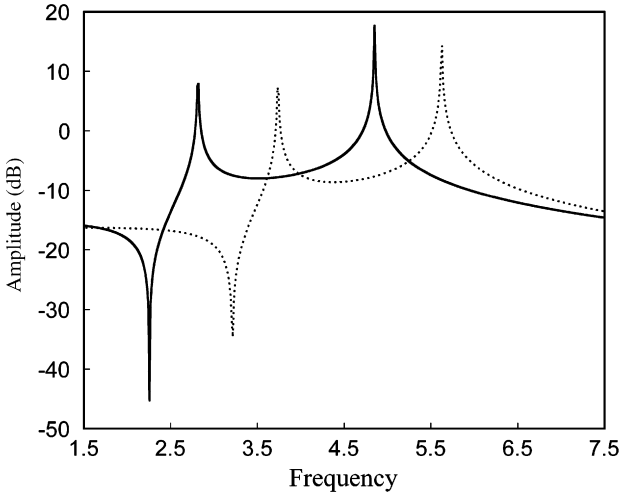

Fig. 6. Frequency response of a drill in drilling process. ····· undrilling, ——— just drilling.

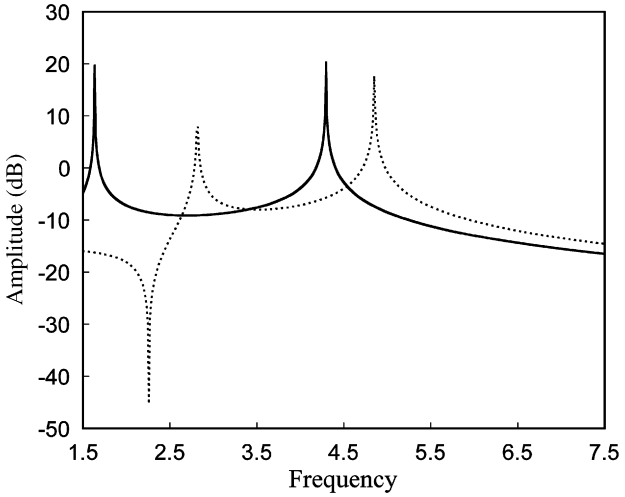

Fig. 7. Frequency response of a drill in drilling process with or without a crack. ····· just drilling without cracks $\gamma = 0.0$, ——— just drilling with a crack $\gamma = 0.3$.

In actual engineering application, the lowest natural frequency is focused to considered, hence, it is also considered to study in this article. The natural frequencies of the drill at different drilling depth when drilling through a work piece are plotted in Fig. 2. In this drilling process, the drill goes into the work piece at time $t = t^* = 0.15$ s. It was found that the natural frequencies of the drill are the same when it is not drilling. The point at which the natural frequencies of the drill decrease suddenly is time $t = t^* = 0.15$ s, drilling depth $\xi(t) = 0^+$. Because a great drilling force acts suddenly, the drill dynamic properties change in the drilling process. In the actual drilling process, a drill that has little vibration prior to work contact can, and often does, vibrate significantly at the instant of contact due to the periodic interactions of the drill periphery with the work piece. This often offsets the hole from the axis of the drill and can have a significant effect on the dynamic behavior and greatly reduce the maximum thrust force that the drill can withstand. After the drill penetrates the work piece, drilling depth $\xi(t) > 0^+$, the natural frequencies of the drill increase as the drilling time increases. In an actual drilling process, the stiffness of the drill changes from weak to strong as the drilling time increases. At the time $t = t^{**} = 0.45$ s, the drill exactly goes throughout the work piece. The natural frequencies of the drill increase suddenly at the time $t = t^{**} = 0.45$ s are observed. Natural frequencies in drilling process remain almost constant after the time $t > t^{**}$.

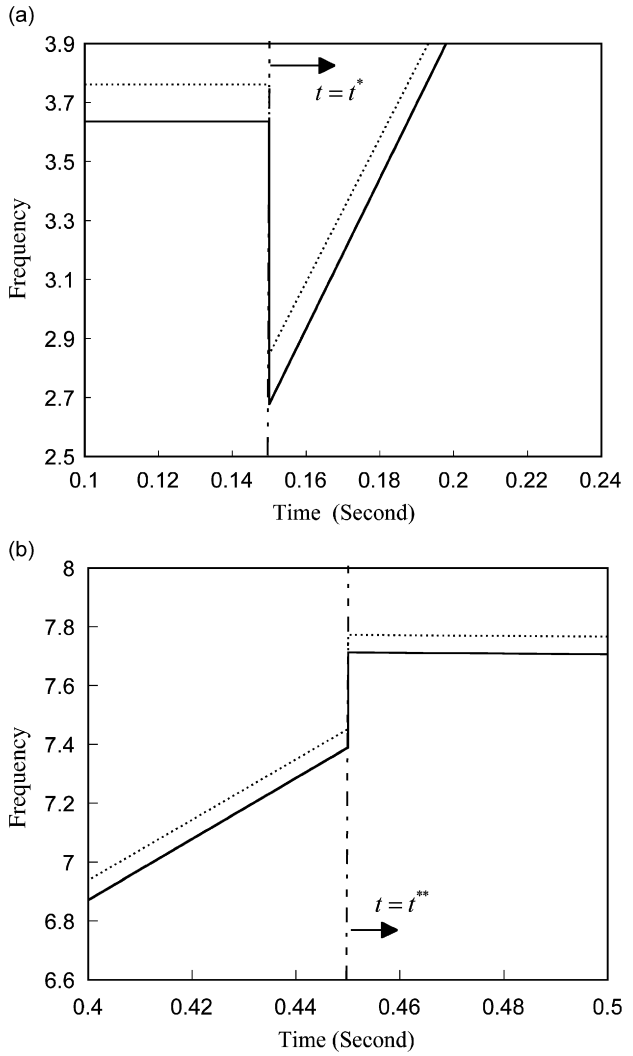

Fig. 8. The variation in natural frequencies when drilling at different spinning speeds: (a) drilling into a work piece and (b) drilling throughout a work piece. ····· rotational speed $\bar{\Omega} = 0.25$, ——— rotational speed $\bar{\Omega} = 1.0$.

Fig. 3 illustrates the natural frequencies of a drill with or without a crack in a drilling process. The crack effect when drilling into a work piece is shown in Fig. 3(a). It is found that the natural frequencies in drilling into a work piece decrease in a drill with a crack. For the same reason, when drilling through a work piece, the natural frequencies are also decreased if this drill has a crack, shown in Fig. 3(b). The variation in the lowest natural frequency of a drill with different crack depths when the drill is undrilling or drilling into a work piece are displayed in Fig. 4. The lowest natural frequency of the drill decreases as the crack depth is increased, whether the drill is drilling into a work piece or not. It is interesting to know the vibration amplitude of a drill with a crack in a drilling process. The dynamic time response in drilling process is illustrated in Fig. 5. A non-dimensional vibration amplitude is employed to display this figure. A large amplitude response occurs at $t = t^* = 0.15$ s, drilling depth $\xi(t) = 0^+$, displayed in Fig. 5(a), the time that the drill goes into the work piece. After the drill is in the work piece, the amplitude response of the drill becomes depressed. Fig. 5(b) shows the dynamic frequency response in a drill with a crack. The results indicate that the vibration amplitude of a drill with a crack is much larger than that without a crack. This would lead to drill breakage.

The frequency response of a drill while undrilling or drilling is illustrated in Fig. 6. The amplitude peak is shifted toward a lower frequency domain as the drill is exactly drilling into a work piece. This phenomenon

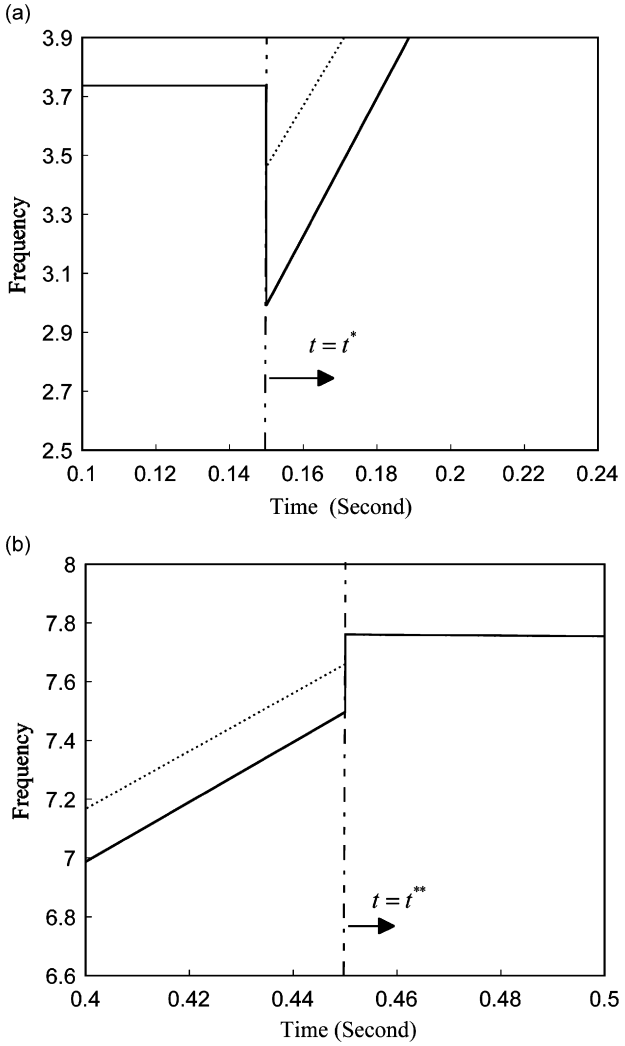

Fig. 9. The variation in natural frequencies in drilling with different thrust forces: (a) drilling into a work piece and (b) drilling throughout a work piece. ····· drilling force $P = 1000$ N, ——— drilling force $P = 2500$ N.

coincides with the previous results as shown in Fig. 2. Fig. 7 shows the frequency response of a drill with or without a crack at time $t = t^* = 0.15$ s. It was found that the amplitude peak shifts further toward a lower frequency domain at time $t = t^* = 0.15$ s if the drill has a crack. The variation in natural frequency when drilling at different rotational speeds is plotted in Fig. 8. In the drilling process, the first natural frequencies of the drill are depressed as the rotational speed increases. In other words, the dynamic characteristics of the drill move from strong to weak if only the rotational speed is increased. With or without work piece interactions, the natural frequencies of a drill are decreased as the rotational speed is increased. The results indicate that a high rotation speed could markedly change the drill dynamics when drilling through a work piece. The thrust force effect may affect the dynamic properties. This thrust force effect on the natural frequencies is shown in Fig. 9. That the natural frequencies of the drill without drilling are independent of the thrust force is observed. However, the dynamic characteristics of a drill will change significantly when drilling through a work piece. The natural frequencies when drilling into a work piece are reduced as the thrust force increases. The effect of the pre-twisted drill angle is considered. Fig. 10 displays the variations in natural frequencies when drilling with different pre-twisted angles. The first natural frequency in the drilling process increases as the pre-twisted angle increases.

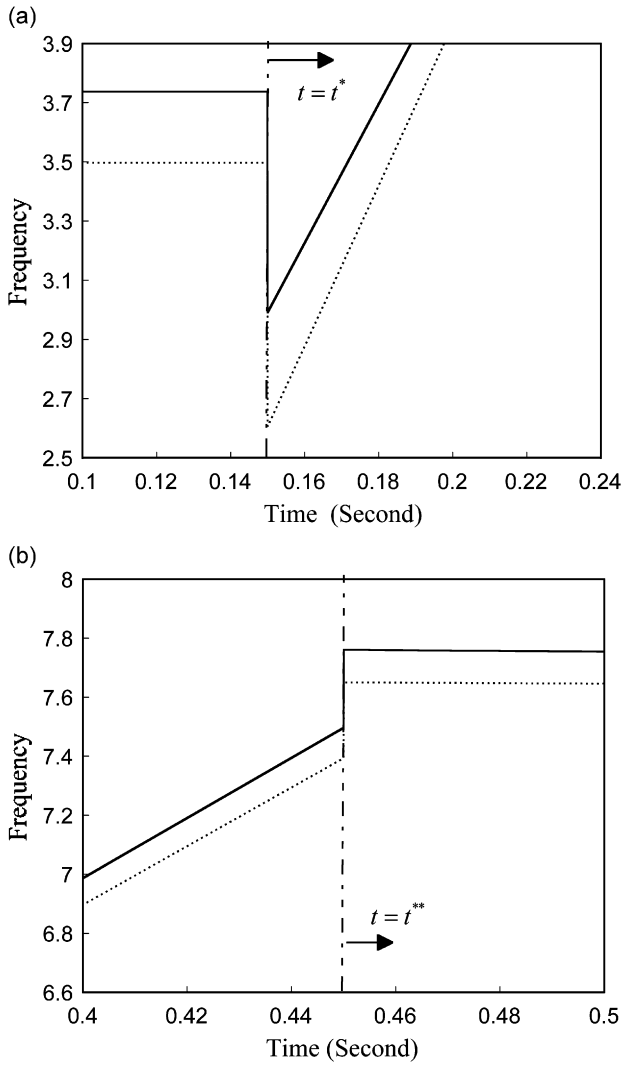

Fig. 10. The variation in natural frequencies in drilling with different pre-twisted angles: (a) drilling into a work piece and (b) drilling throughout a work piece. ····· pre-twisted angle $\beta = 7.8539$ rad/m, ——— pre-twisted angle $\beta = 31.4159$ rad/m.

4. Conclusions

A dynamic model for the drill in the time dependent drilling process is proposed. The effects of different drilling parameters on the vibration of a drill during the drilling process are investigated. The effect of a local crack on the drill vibration has also been discussed. The major conclusions drawn from the analysis and numerical results obtained in this study are summarized as follows:

(1) A serious drill vibration is observed as the drill just start to drill in a work piece. The existence of a local crack may aggravate the drill vibration seriously.
(2) The simulated results indicate that the natural frequencies of the drill are changed significantly during the drilling process.
(3) The lowest natural frequency of a drill decreases with the increase of the drilling force. The results simulated from the proposed dynamic model also indicate that the rotation speed and pre-twisted angle may change the drilling vibration drastically.

Acknowledgments

The author would like to thank the National Science Council, Taiwan, Republic of China, for financially supporting this research through Grant NSC 95-2221-E-230-006.

Appendix A

By employing Euler–Bernoulli beam theory, the equation of motion of a pre-twisted beam, a drill, can be derived [29]. The displacement field at any point in the cross-section in a rotating coordinate system xyr can be expressed as

$$U_r = -x\frac{\partial u}{\partial r} - y\frac{\partial v}{\partial r} \tag{A.1}$$

$$U_x = u(r,t) \tag{A.2}$$

$$U_y = v(r,t) \tag{A.3}$$

As above, the strain energy can be also derived as

$$U = \frac{1}{2}\int_v \sigma_r \varepsilon_r \,\mathrm{d}v \tag{A.4}$$

$$U = \frac{1}{2}\int_0^L \left[EI_{yy}\left(\frac{\partial^2 u}{\partial r^2}\right)^2 + 2EI_{xy}\frac{\partial^2 u}{\partial r^2}\frac{\partial^2 v}{\partial r^2} + EI_{xx}\left(\frac{\partial^2 v}{\partial r^2}\right)^2\right]\mathrm{d}r \tag{A.5}$$

The velocity field at any point in the cross-section is displayed as

$$\dot{U}_r = -x\frac{\partial^2 u}{\partial t \partial r} - y\frac{\partial^2 v}{\partial t \partial r} \tag{A.6}$$

$$\dot{U}_x = \frac{\partial u}{\partial t} - v\Omega - y\Omega \tag{A.7}$$

$$\dot{U}_y = \frac{\partial v}{\partial t} + u\Omega + x\Omega \tag{A.8}$$

The kinetic energy of system is displayed as

$$T = \int_v \rho(\dot{U}_r + \dot{U}_x + \dot{U}_y)\,\mathrm{d}v \tag{A.9}$$

Substituting Eqs. (A.6)–(A.8) into Eq. (A.9), the kinetic energy is

$$T = \int_0^L \left[\bar{I}_{yy}\left(\frac{\partial^2 u}{\partial t \partial r}\right)^2 + 2\bar{I}_{xy}\frac{\partial^2 u}{\partial t \partial r}\frac{\partial^2 v}{\partial t \partial r} + \bar{I}_{xx}\left(\frac{\partial^2 v}{\partial t \partial r}\right)^2 + \mu\left[\left(\frac{\partial u}{\partial t}\right)^2 + \left(\frac{\partial v}{\partial t}\right)^2\right]\left(\frac{\partial u}{\partial t}\right)^2 + \mu\Omega^2(u^2+v^2) - 2\mu\Omega\frac{\partial u}{\partial t}v + 2\mu\Omega\frac{\partial v}{\partial t}u - \Omega^2\bar{I}_{rr}xx\left(\frac{\partial^2 u}{\partial t \partial r}\right)^2 xx\right] \mathrm{d}r \tag{A.10}$$

The Hamilton's principle is employed in this work. It is

$$\int_{t_1}^{t_2} \delta(T-U)\,\mathrm{d}t = 0 \tag{A.11}$$

Substituting Eqs. (A.5) and (A.10) into the above equation and performing the necessary integrations by parts, the equation of motion and associated boundary conditions can be derived. The equation of motion for the drill body is given by

$$\frac{\partial^2}{\partial r^2}\left(EI_{yy}\frac{\partial^2 u}{\partial r^2} + EI_{xy}\frac{\partial^2 v}{\partial r^2}\right) - \frac{\partial}{\partial r}\left(\bar{I}_{yy}\frac{\partial^3 u}{\partial t^2 \partial r} + \bar{I}_{xy}\frac{\partial^3 v}{\partial t^2 \partial r}\right) + \mu\frac{\partial^2 u}{\partial t^2} - 2\mu\Omega\frac{\partial v}{\partial t} - \mu\Omega^2 u = 0 \tag{A.12}$$

$$\frac{\partial^2}{\partial r^2}\left(EI_{xx}\frac{\partial^2 v}{\partial r^2} + EI_{xy}\frac{\partial^2 u}{\partial r^2}\right) - \frac{\partial}{\partial r}\left(\bar{I}_{xx}\frac{\partial^3 v}{\partial t^2 \partial r} + \bar{I}_{xy}\frac{\partial^3 u}{\partial t^2 \partial r}\right) + \mu\frac{\partial^2 v}{\partial t^2} + 2\mu\Omega\frac{\partial u}{\partial t} - \mu\Omega^2 v = 0 \tag{A.13}$$

The corresponding boundary conditions are

$$\delta\left(\frac{\partial u}{\partial r}\right) = 0 \quad \text{or} \quad EI_{yy}\frac{\partial^2 u}{\partial r^2} + EI_{xy}\frac{\partial^2 v}{\partial r^2} = 0 \tag{A.14}$$

$$\delta\left(\frac{\partial v}{\partial r}\right) = 0 \quad \text{or} \quad EI_{xx}\frac{\partial^2 v}{\partial r^2} + EI_{xy}\frac{\partial^2 u}{\partial r^2} = 0 \tag{A.15}$$

$$\delta u = 0 \quad \text{or} \quad \bar{I}_{yy}\frac{\partial^3 u}{\partial t^2 \partial r} + \bar{I}_{xy}\frac{\partial^3 v}{\partial t^2 \partial r} - \frac{\partial}{\partial r}\left(EI_{yy}\frac{\partial^2 u}{\partial r^2} + EI_{xy}\frac{\partial^2 v}{\partial r^2}\right) = 0 \tag{A.16}$$

$$\delta v = 0 \quad \text{or} \quad \bar{I}_{xx}\frac{\partial^3 v}{\partial t^2 \partial r} + \bar{I}_{xy}\frac{\partial^3 u}{\partial t^2 \partial r} - \frac{\partial}{\partial r}\left(EI_{xx}\frac{\partial^2 v}{\partial r^2} + EI_{xy}\frac{\partial^2 u}{\partial r^2}\right) = 0 \tag{A.17}$$

References

[1] M. Shaw, *Metal Cutting Principles*, Clarendon Press, Oxford, 1989.

[2] D.D. Rosard, Natural frequency of twisted cantilever beams, *ASME, Journal of Applied Mechanics* 20 (1953) 241–248.

[3] G.W. Jarrett, P.C. Warner, The vibration of rotating tapered twisted beam, *ASME, Journal of Applied Mechanics* 20 (1953) 381–389.

[4] O. Tekinalp, A.G. Ulsoy, Modeling and finite element analysis of drill bit vibration, *ASME, Journal of Vibration, Acoustics, Stress, and Reliability in Design* 111 (1989) 148–155.

[5] O. Tekinalp, A.G. Ulsoy, Effect of geometric and process parameters in drill transverse vibration, *ASME, Journal of Engineering for Industry* 112 (1990) 189–194.

[6] C.L. Liao, Y.H. Dang, Structural characteristics of spinning pretwisted orthotropic beams, *Computers & Structures* 45 (4) (1992) 715–731.

[7] C.L. Liao, B.W. Huang, Parametric instability of a pretwisted beam under periodic axial force, *International Journal of Mechanical Science* 37 (4) (1995) 423–439.

[8] E. Magrab, D.E. Gilsinn, Bucking loads and natural frequency of twist drills, *Transactions of ASME* 106 (1984) 196–204.

[9] A.G. Ulsoy, A lumped parameter model for the transverse vibration of drill bit, *Control of Manufacturing Processes and Robotic System* (1989) 15–25.

[10] H. Fuji, E. Marui, S. Ema, Whirling vibration in drilling part 3: vibration analysis in drilling workpiece with a pilot hole, *ASME, Journal of Engineering for Industry* 110 (1988) 315–321.

[11] K. Fuenkajorn, J. Daemen, Drilling-induced fractures in borehole walls, *International Journal of Rock Mechanics and Mining Sciences & Geomechanics Abstracts* 29 (5) (1992) 307.
[12] A. Mohamed, A. Ragab, On blunting the crack tip through hole-drilling, *Alexandria Engineering Journal* 42 (3) (2003) 347–355.
[13] B.J. Park, Y.J. Choi, C.N. Chu, Prevention of exit crack in micro drilling of soda-lime glass, *CIRP Annals—Manufacturing Technology* 51 (1) (2002) 347–350.
[14] J.B. Shu, X.M. Deng, L.Q. Xu, Cracking reason analysis on the 35CrMo steel drill in forging process, *Heat Treatment of Metals* 29 (8) (2004) 72 (in Chinese).
[15] P.F. Rizos, N. Aspragathos, A.D. Dimarogonas, Identification of crack location and magnitude in a cantilever beam from the vibration mode, *Journal of Sound and Vibration* 138 (1990) 381–388.
[16] D. Broek, *Elementary Engineering Fracture mechanics*, Martinus Nijhoff Publishers, New York, 1986.
[17] H. Tada, P. Paris, G. Irwin, *The Stress Analysis of Crack Handbook*, Del Research Corporation, Hellertown, PA, 1973.
[18] L. Chen, C. Chen, Vibration and stability of cracked thick rotating blade, *Computers & Structures* 28 (1988) 67–74.
[19] B. Grabowski, The vibrational behavior of a turbine rotor containing a transverse crack, *ASME, Journal of Mechanical Design* 102 (1980) 140–146.
[20] G. Sakar, M. Sabuncu, Dynamic stability of a rotating asymmetric cross-section blade subjected to an axial periodic force, *International Journal of Mechanical Sciences* 45 (9) (2003) 1467–1482.
[21] G. Sakar, S. Mustafa, Buckling and dynamic stability of a rotating pretwisted asymmetric cross-section blade subjected to an axial periodic force, *Finite Elements in Analysis and Design* 40 (11) (2004) 1399–1415.
[22] D.M. Rincon, A.G. Ulsoy, Complex geometry, rotary inertia and gyroscopic moment effects on drill vibrations, *Journal of Sound and Vibration* 188 (5) (1995) 701–715.
[23] H.P. Lee, Dynamic response of a beam with a moving mass, *Journal of Sound and Vibration* 192 (2) (1996) 289–294.
[24] Y.M. Ram, J. Caldwell, Free vibration of a string with moving boundary conditions by the method of distorted images, *Journal of Sound and Vibration* 194 (1) (1996) 35–47.
[25] R.F. Fung, J.S. Huang, J.J. Chu, Dynamic stability of an axially traveling string/slider coupling system with moving boundary, *Journal of Sound and Vibration* 211 (4) (1998) 689–701.
[26] S.S. Law, X.Q. Zhu, Study on different beam models in moving force identification, *Journal of Sound and Vibration* 234 (4) (2000) 661–679.
[27] J.S. Wu, D.W. Chen, Dynamic analysis of a uniform cantilever beam carrying a number of elastically mounted point masses with dampers, *Journal of Sound and Vibration* 229 (3) (2000) 549–578.
[28] B.W. Huang, Dynamic characteristics of a drill in drilling process, *IMechE, Part B, Journal of Engineering Manufacture* 217 (2003) 161–167.
[29] C.L. Liao, B.W. Huang, Parametric resonance of a spinning pretwisted beam with time-dependent, *Journal of Sound and Vibration* 180 (1) (1995) 47–65.
[30] M. Swaminathan, J.S. Rao, Vibration of rotating pretwisted and tapered blades, *Mechanism and Machine Theory* 12 (1977) 331–337.
[31] J.S. Rao, Flexural vibration of pretwisted tapered cantilever blades, *ASME, Journal of Engineering for Industry* (1972) 343–346.
[32] A.D. Dimarogonas, S.A. Paipetis, *Analytical Methods in Rotor Dynamics*, Applied Science Publishers, New York, 1983.
[33] M. Krawczuk, W.M. Ostachowicz, Transverse natural vibrations of a cracked beam loaded with a constant axial force, *ASME, Journal of Vibration and Acoustics* 115 (1993) 524–528.
[34] .H.P. Lee, Dynamic stability of a tapered cantilever beam on an elastic foundation subjected to a follower force, *International Journal of Solids and Structures* 33 (10) (1996) 1409–1424.
[35] B.W. Huang, H.K. Kung, W.L. Yao, Effect of periodic drilling force on instability in a drilling process, *IMechE, Part C, Journal of Mechanical Engineering Science* 219 (8) (2005) 733–742.